A NUMERICAL ANALYSIS OF THE PROCESS OF CAPTURE INTO RESONANCE

RODNEY S. GOMES AND ALEXANDRE Y. MIGUELOTE
Observatório Nacional
Rua General José Cristino, 77 CEP 20921-400 Rio de Janeiro, RJ - Brazil

The process of capture into a mean motion resonance induced by a non conservative force has been studied by many authors (Henrard,1982); Peale,1986). Capture probabilities have been established through the use of an analytical model based on averaged Hamiltonian systems, with an adiabatic varying parameter (Henrard, 1982; Lemaitre,1984). For each resonance, these probabilities are basically function of the orbital element involved (eccentricity and/or orbital inclination) far from the resonance and the perturber's mass, there being no dependence on the dissipation rate. However when the process is not adiabatic, the dissipation rate has a fundamental importance for capture probabilities (Gomes,1995). For these processes, an analytical association of orbital elements far from the resonance with capture probabilities is still an open question. Association of orbital elements just before resonance with the process of capture is presented in (Marzari and Vanzani, 1994) and (Lazzaro et al, 1994). In these works the eccentricity and longitude of the perihelion are checked for in respect with capture into resonance. Here we aim at verifying how the trapping process changes with orbital elements just before resonance, but not restricting ourselves to the pair eccentricity-perihelion.

We choose Poynting-Robertson drag (with $\beta = 0.01$ unless otherwise stated) as the dissipative force and the 2:3 resonance with a circular orbit Earth ($a_{res} \cong 1.306$). The particle is on the Earth's orbital plane.

Figure 1 shows the result coming from the integration of 60 particles, starting with $a = 1.31014, e = 0.05$ and $\varpi = 0$. The initial mean longitudes are uniformly distributed from 0° to 120°. The figure plots initial mean longitudes against semimajor axes after 1200 years. The abrupt increase of the semimajor axes for initial longitudes from 64° to 120° and 0° to 4° indicates which particles are trapped in the 2:3 resonance with the Earth.

S. Ferraz-Mello et al. (eds.), Dynamics, Ephemerides and Astrometry of the Solar System, 223–228.

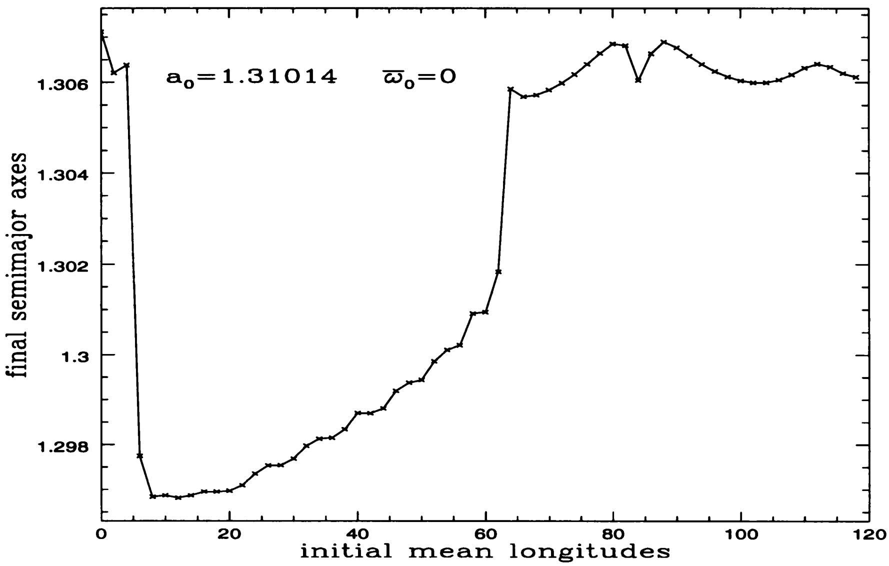

Figure 1.
Initial mean longitudes against semimajor axes after 1200 *years numerical integration of the orbits of 60 particles subject to Poynting-Robertson drag* (β = 0.01)*, started just above the 2:3 resonance with the Earth. Other elements are* $a = 1.31014$*,* $e = 0.05$ *and* $\varpi = 0°$*, for all particles.*

We see that near the resonance there is a continuous range of mean longitudes associated to particles that are trapped (this feature is not however observed in all cases. Some examples show this longitude region split into two). For initial mean longitudes from 120° to 360° this same configuration will repeat itself twice, what is expected from the fact that the resonant angle $\phi = 3\lambda - 2\lambda_T - \varpi$ varies 3 times as fast as λ.

For our next experiment, we slightly change the initial semimajor axis ($a = 1.31023$), other conditions being the same as those of figure 1. Figure 2 shows which particles are trapped for this different initial semimajor axis. The first conclusion we may draw from this figure is that there is no point in taking capture probabilities from the results shown in figure 1, because the number of trapped particles varies considerably with the semimajor axis. This last result almost unavoidably yields our next experiment, which is plotting the number of trapped particles against their initial semimajor axes. This is shown in figure 3. Here we notice peaks of relatively high number of trapped particles between valleys of relatively low number of trapped particles. For an interpretation of this diagram, we first measure

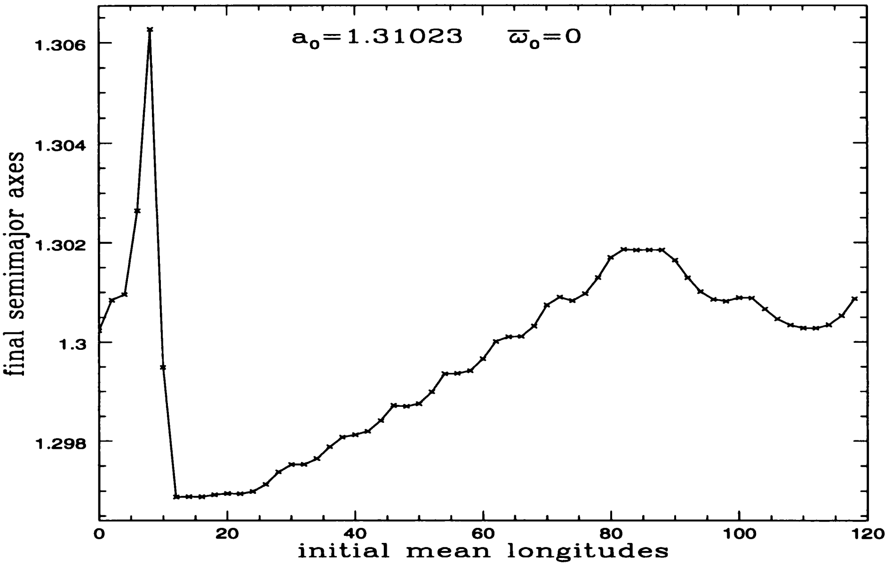

Figure 2.
Like figure 1, for another initial semimajor axis (a = 1.31023*). The number of trapped particles is quite different from that of figure 1.*

the distance between successive peaks. This distance is not constant and it is not difficult to verify that it refers to the variation of the semimajor axis due to the Poynting-Robertson dissipation in a ϕ-period. We postpone a better explanation of this point after we analyze our next experiment.

Figures 4a and 4b show the evolution of the resonant angles ϕ at every 10 years from an initial uniform distribution through 360°. These figures suggest another reason why figure 1 is not suitable to give capture probabilities. In fact, near a resonance, the initial uniform distribution of ϕ on a circle is artificial. After a short time the particles resonant angle accumulate near a point, due to the fact that $\dot{\phi}$ has a relative high variation near $\dot{\phi} = 0$. Figure 4a refers to an initial semimajor axis ($a = 1.31014$) (same as Figure 1), which generated high number of captured particles, whereas figure 4b refers to $a = 1.31023$ (same as Figure 2) and just one particle is captured. These figures suggest that the value of ϕ where $\dot{\phi} = 0$ for the first time is related to whether the particle is going to be captured or not. So these last two conclusions taken from figures 4a and 4b lead us to an explanation of figure 3. The fact that the resonant angles get and run together near a resonance associated to the fact that these angles will have their time derivative vanishing in a region that leads or not to capture gives a good explanation for the peaks and valleys of figure 3.

https://doi.org/10.1017/S0074180900127421 Published online by Cambridge University Press

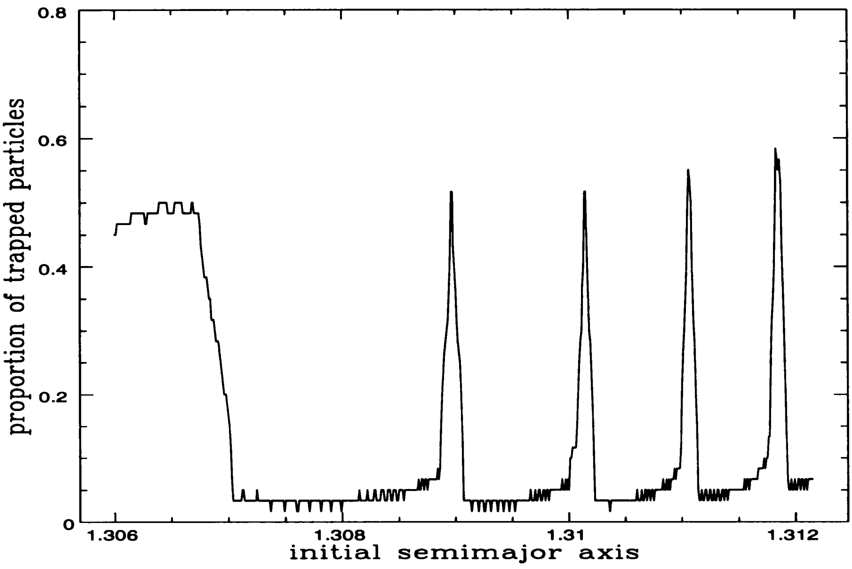

Figure 3.
Proportion of trapped particles against initial semimajor axis, all other initial orbital elements like those of figure 1.

Our last numerical experiment tries to better understand the association of a region of eccentricities and resonant angles where $\dot{\phi} = 0$ for the first time (return points) with capture or non capture. Figure 5 shows (P, ϕ) points, where $P = na^2(1 - \sqrt{1 - e^2})$, associated to the time when $\dot{\phi} = 0$ for the first time. Larger dots belong to captured particles and the smaller ones belong to non captured particles. We start the integrations with sets of equal eccentricities and different semimajor axes. These elements vary from a minimum value associated to an early separatrix crossing (near 360°) to a maximum value associated to a late separatrix crossing (near 0°), but the separatrix crossing occurs always before a complete turn of the angle ϕ (note that the motion is clockwise). For each eccentricity, the return points lie in approximate arcs of circles as the semimajor axis varies. Here we use several values of β. Smaller β approximate the adiabatic case. We notice here that some general ideas given by the theory for the adiabatic case are also present in the non adiabatic case. Reminding the analytical model (Henrard,1982; Peale,1986), captured particles cross the separatrix early, so that they have time to get the lowest possible energy level before they start to have their resonant angles running in the opposite way. $\dot{\phi} = 0$ in the lowest levels of energy means $\dot{\phi} = 0$ for the highest values of ϕ, as found in

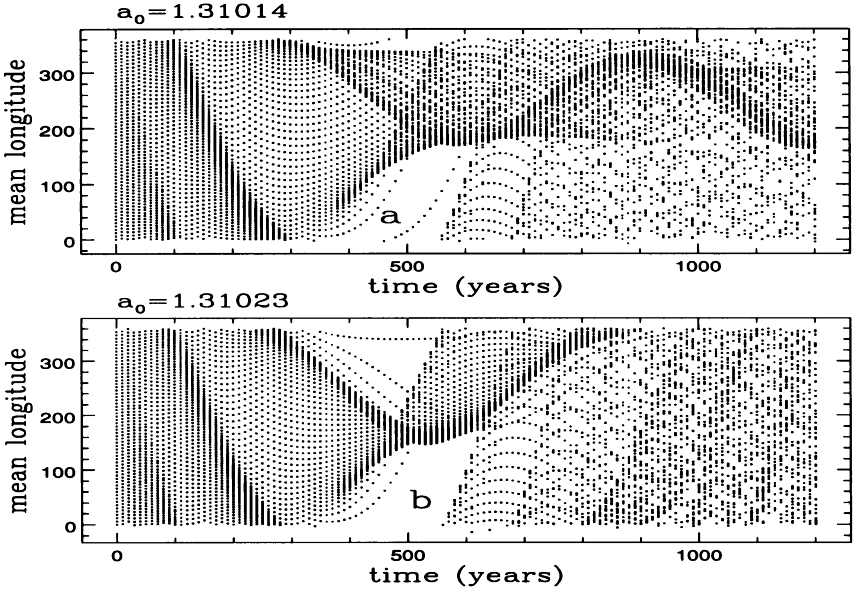

Figure 4.
Evolution of the mean longitudes at every 10 years for 60 particles. (a) the same conditions as in figure 1. (b) the same conditions as in figure 2.

every plotting for low and high β. When we get closer to the adiabatic case (lower β) the return points are closer to 0° as a whole. This is explained by the fact that $\frac{d(H-H^*)}{dt}$, where H is the Hamiltonian associated to the evolving orbit and H^* is the Hamiltonian associated to the separatrix, is proportional to β. Thus, for small β, the return point belongs to a libration curve near the separatrix. These curves have return points near 0°. We also see the variation of the number of captured particles with eccentricity, which for the adiabatic case is higher as smaller is the eccentricity and for faster dissipation there is a peak of highest capture probability away from $e = 0$. This peak is associated to as high e as higher is β, but the height of the peak gets lower itself. These last results confirm (Gomes, 1995).

References

Gomes,R.S.: 1995, 'Resonance trapping and evolution of particles subject to Poynting-Robertson drag: adiabatic and non-adiabatic approaches', *Celestial Mechanics and Dynamical Astronomy* **61:1**, pp. 97-113

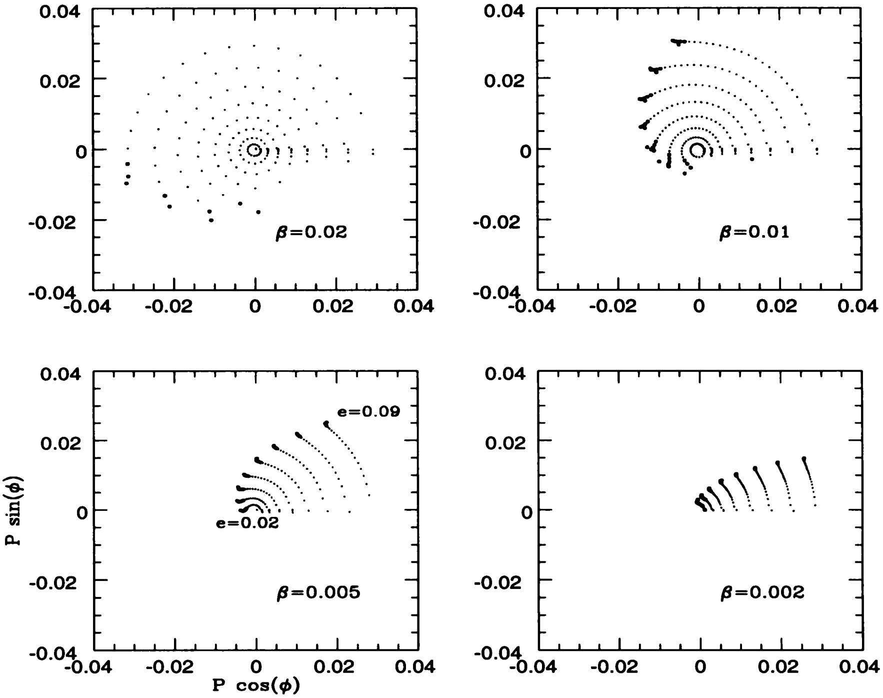

Figure 5.

(P, ϕ) points where $\dot{\phi} = 0$ for the first time, for several initial eccentricities and several β. In each figure the eccentricity varies from 0.02 to 0.09. The return points associated to resonance trapping are printed larger. For each β and e, the several points located on approximate arcs of circles correspond to different initial semimajor axes. All integrations start with $\phi = 0$ ($\lambda = 0$, $\varpi = 0$ and $\lambda_T = 0$).

Henrard,K.: 1982, ' Capture into resonance: an extension of the use of adiabatic invariants', *Celestial Mechanics* **27**, pp. 3-22

Lazzaro,D., Sicardy,B., Roques,F., Greenberg,R.: 1994, 'Is there a planet around β Pictoris? Perturbations of a planet on a circumstellar dust disk.', *Icarus* **108**, pp. 59-80

Lemaitre,A.: 1984, 'High-order resonances in the restricted 3-body problem.', *Celestial Mechanics* **32**, pp. 109-126

Marzari,F. and V.Vanzani: 1994, 'Dynamical evolution of interplanetary dust particles.', *Astron. & Astrophys.* **283**, pp. 275-286

Peale,S.J.: 1986, 'Orbital resonances, unusual configurations and exotic rotation states among planetary satellites.' *in Satellites (eds. Burns, J.A. and Mathews, M.S.), University of Arizona Press* pp. 159-223